

Analytical fragility curves of a structure subject to tsunami waves using smooth particle hydrodynamics

Fritz Sihombing^a and Marco Torbol^{*}

Ulsan National Institute of Science and Technology (UNIST), Ulsan, Republic of Korea

(Received September 16, 2015, Revised August 20, 2016, Accepted August 23, 2016)

Abstract. This study presents a new method to compute analytical fragility curves of a structure subject to tsunami waves. The method uses dynamic analysis at each stage of the computation. First, the smooth particle hydrodynamics (SPH) model simulates the propagation of the tsunami waves from shallow water to their impact on the target structure. The advantage of SPH over mesh based methods is its capability to model wave surface interaction when large deformations are involved, such as the impact of water on a structure. Although SPH is computationally more expensive than mesh based method, nowadays the advent of parallel computing on general purpose graphic processing unit overcome this limitation. Then, the impact force is applied to a finite element model of the structure and its dynamic non-linear response is computed. When a data-set of tsunami waves is used analytical fragility curves can be computed. This study proves it is possible to obtain the response of a structure to a tsunami wave using state of the art dynamic models in every stage of the computation at an affordable cost.

Keywords: reliability analysis; smooth particle hydrodynamics; structural dynamics; parallel computing; GPGPU computing; CUDA

1. Introduction

A tsunami can reach the same magnitude of destructive power of an earthquake. Example of recent tsunamis are: the 2011 Tohoku earthquake and tsunami (Mori, Takahashi *et al.* 2011), which caused the meltdown of the Fukushima Daiichi nuclear power plant and destruction over a large area along the east coast of Japan, the 2010 Sumatra earthquake and tsunami (Hill, Borrero *et al.* 2012), and the 2004 Indian ocean tsunami (Borrero 2005, Wang and Liu 2006), which killed more than 230,000 people.

2004 Sumatra earthquake was one of the largest earthquake in last 40 years. The recorded magnitude was $M_w = 9.0$, the aftershocks occurred in the fault line as long as 1200 km, the affected area of fault was estimated roughly around 200 km wide, with slips of 10 m (Wang and Liu 2006). The earthquake generated massive and catastrophic tsunami waves. In the Banda Aceh, the western side of northern part of Sumatra, the tsunami wave inundate land as far as 3 to 4 km from the coastline with the tsunami wave run-up as high as 31 m. The tsunami flooded an area as wide

^{*}Corresponding author, Assistant Professor, E-mail: mtorbol@unist.ac.kr

^a Graduate student, E-mail: fritzharland@unist.ac.kr

as 65 km² between Banda Aceh and Lhoknga district as found in Borrero (2005).

Tohoku 2011 earthquake occurred on March 2011, the magnitude of earthquake was $M_w=9.0$ and located in the Pacific coast of Japan. The tsunami wave was generated 130 km off Miyagi Prefecture coast and reached the coastline 20 minutes after the earthquake first shock, the tsunami affected 2000 km of coastal area. The maximum recorded run-up height was 39.7 m at Miyako area and reached 290 km at inland width a run-up height greater than 20 m (Mori, Takahashi *et al.* 2011).

Up to nowadays, the propagation of tsunami waves over the ocean was simulated using mesh based methods, such as: finite differences of finite element methods (FEM). However, this method does not compute the impact force of a wave on the surface of the structures, such as buildings or bridges. In addition, even though the height of the wave at the location of the structure can be recorded and equations exist to compute equivalent static impact forces (Dao, Xu *et al.* 2013), there is not a direct relation between the time history of the height of the wave and the impact force. If the impact forces could be recorded inside the tsunami model, FEM non-linear dynamic analysis of the structure could be performed to obtain the accurate structural responses. Nowadays, different methods exist to simulate the interaction between a wave and a surface, and mesh-less methods are the most promising. Smooth particle hydrodynamics (SPH) method is one example of mesh-less method (Gingold and Monaghan 1977, Barreiro, Crespo *et al.* 2013, St-Germain, Nistor *et al.* 2014, Altomare, Crespo *et al.* 2015).

In this study, the SPH method (Gingold and Monaghan 1977) is used to simulate the propagation of the tsunami waves from shallow water to the location of the structure. SPH is a mesh-less method used in computational fluid dynamics. The concept is not new but SPH was always computationally too expensive for the computational power available than mesh based FEM, and up to now it either required large scale supercomputers or it was limited to small scale problems. The rise of general purpose graphic processing unit (GPGPU) allowed the use of SPH for the large scale simulation on desktop computers and workstations equipped with graphic processing units (GPUs).

The simulation of tsunami waves are performed using DualSPHysics (Crespo, Domínguez *et al.* 2015). DualSPHysics is developed on C++, CUDA, and Java codes and it is used to understand the behavior of fluid particle especially on the free-surface flow phenomena. For example evaluation of armor block sea breakwater response due to wave breaking (Altomare, Crespo *et al.* 2014) and to evaluation of wave impact on storm return walls (Altomare, Crespo *et al.* 2015). In this study, DualSPHysics is used to simulate the impact of tsunami waves on two prototype 3-storey reinforced concrete structures.

A data-set of 96 tsunami waves is built and 96 SPH simulations are performed to obtain the time histories of the impact forces on the structure. The capacity of the structure is computed using non-linear static analysis. Moment-curvature analysis is used to evaluate the capacity of the cross-sections subject to bending moment and axial forces. Push-over analysis is used to evaluate the capacity of the columns subject to shear force. The demand is computed using non-linear dynamic analysis where the time histories of the impact force which is the output of the SPH simulation are the input forces. Capacity and demand are compared to assess the damage state of the structure and to calculate its analytical fragility curves. Fragility curves represent the failure probability or damage probability of a structure due to a certain event (Schultz, Gouldby *et al.* 2010). Fragility curves can be computed based on judgmental observation, empirical method, analytical method like in this study, and hybrid method.

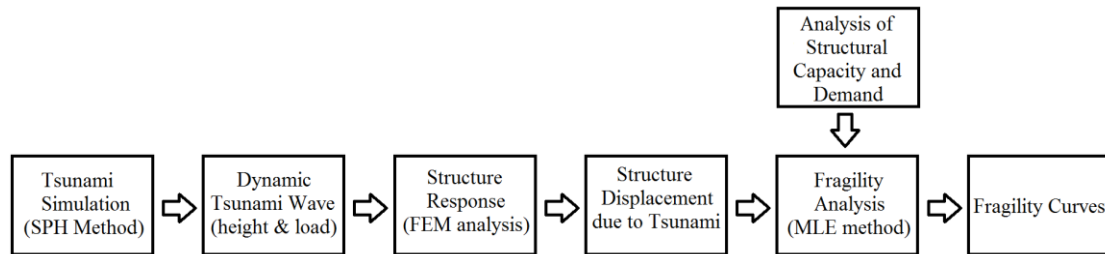


Fig. 1 Dynamic tsunami analysis fragility curves flowchart

2. Methodology

The method developed in this study to compute analytical fragility curves of buildings subject to tsunami waves is shown in Fig. 1. First the smoothed particle hydrodynamic (SPH) method simulates the tsunami waves based on the given boundary conditions. The tsunami wave height evolution and the exerted force on the structure due to the impact of wave are recorded in every time step of the simulations. Second, a finite element model of the structure is built and its structural response is calculated using nonlinear dynamic analysis. The parameters of the fragility curves are computed using the responses from a data set of tsunami scenarios. The fragility curves show the probability of exceeding a given damage state as a function of a chosen tsunami intensity measure (IM). In earthquake engineering many well defined IM exist, such as: PGA, PGV, PGD, $S_a(W_1)$, $S_v(W_1)$, $S_d(W_1)$ and many others. On the other hand, the intensity measures of tsunami wave are not well defined. In this study, the intensity measures are: the tsunami wave height arriving at the coastline and the tsunami wave height at the structure.

2.1 Tsunami event

Tsunami is a word borrowed from Japanese language, it is derives from two words: “tsu” harbor and “nami” wave. In the beginning the word tsunami was only known to scientist and those who dealt with disaster. However, the name gained global recognition when the occurrence of events caused catastrophic results, such as: Aceh-Indian Ocean Tsunami in 2004, Pangandaran Tsunami in 2006, and Tohoku Tsunami in 2011.

The tsunami is series of waves caused by a disturbance in the sea. The sources of this disturbance are: underwater earthquake, surface/submarine landslides, volcanic eruptions and underwater gas emission. Furthermore, meteorological activities can cause tsunami waves, i.e. meteorological tsunami. A submarine earthquake is the most common source of tsunami waves but not all submarine earthquakes generate tsunami waves. Earthquakes along thrust-type faults can cause a vertical movement of the sea floor that will induce a disturbance on the body of water located above it. The waves generated from this event tend to be tsunamigenic. Another type of earthquake is the earthquakes along normal-type faults which can cause tsunami waves of moderate intensity, while earthquakes from strike-slip type faults do not cause tsunami waves. If the sea floor disturbance induces a displacement of a large volume of water instantaneously and it will generate tsunami waves on the sea surface. Tsunami waves are different from wind-generated waves. Wind-generated waves have period of around 10 seconds and wave length of around 150 m.

Instead, tsunami waves have period of up to 1 hour and wave length up to 100 km. Because of these properties detecting a tsunami wave in the open ocean is difficult.

Another source of sea disturbance is surface/submarine landslides. These landslides are triggered by earthquakes, storm waves, and rapid sedimentation. The properties of the tsunami waves generated by submarine landslides are function of the sea floor topography and the slide rheology. The steeper topography of sea floor the chance of sediment collapse is bigger and the stiffer the slide material the amount of energy that can be converted into tsunami energy is decreased (Gisler, Weaver *et al.* 2010). The mechanism of wave formation and wave propagation of surface/submarine-landslide-generate-tsunami is divided in: landslide dynamics, energy transfer, wave propagation on the surface, and run-up wave on the coastline (Horbitz, Lovholt *et al.* 2006). Both surface and submarine landslides can generate tsunami waves but surface landslides that enter the water over a large area and at high speed have higher chance of generating tsunami waves than slow moving submarine landslide (Joseph 2011). Moreover, a tsunami wave generated by a surface/submarine landslide has higher amplitude and higher run-up close to its point of origin (Mohammed and Fritz 2010).

A tsunami wave is classified based on different properties: the distance between its point of origin and the coastline, the wavelength and the wave speed. The distance between the point of origin source and the coastline defines if a tsunami is: far-field, where the distance is more than 1,000 km, or a near-field, where the distance is less than 200 km (National Tsunami Warning 2014). The wavelength of tsunami can be varied from 10 km in shallow water to 500 km in the open ocean. Lastly, the wave speed of tsunami is given by Eq. (1) (National Tsunami Warning 2014).

$$v = \sqrt{h_w \cdot g} \quad (1)$$

where h_w is the depth of the water and g is the gravity acceleration.

In the open ocean, it can be difficult to observe the tsunami waves because they have long period, long wavelength and small amplitude. Instead, when the tsunami waves reach the coastline the wavelength shortens and the wave height increases suddenly because the water depth decreases from hundreds of meters to few meters. For these reasons tsunami waves give no warning while approaching and cause disasters on the coastline. Due to its sudden increase in wave height tsunami waves surges and floods the land. In addition, along their path the waves will include sediments that make the water denser and increase the kinetic energy of the waves. When tsunami waves impact on a structure damage will likely occurred and can lead to the collapse of structure. The wave flood the land along with the debris of structures, cars, ships, and vegetation, these are threat for both structures and human life.

Understanding the impact of tsunami waves on structure is one important point on tsunami research field. Post-tsunami field surveys are performed by researchers and scientists to identify the damage created by the impact of tsunami waves. The reports include: tsunami height data, inundation length data, structural damage assessment, and life loss record. These reports are useful to engineers to understand the impact of the tsunami over the area, such as: inundation flow, inundation area, and structural damage. These reports are also used by local authorities to plan for future events and to mitigate the consequences. Due to the local aspect in the data difficulties rise when one has to quantify the damages and the vulnerabilities. To encounter the locality and provide generally measurement of damage, empirical tsunami fragility curves based on survey

reports, were proposed as a method to measure the impact of tsunami waves (Koshimura, Namegaya *et al.* 2009). The tsunami fragility curves are defined as the probability of exceeding a damage state based on an intensity measure of the tsunami wave. The intensity measures taken into consideration are: inundation depth, tsunami current velocity, tsunami's loading force paired with the data of structural damages.

2.2 Static force for Tsunami

The correct estimation of the impact force of tsunami waves is important when performing tsunami risk assessment. The estimation can be done using: empirical method, analytical method, or numerical method. The empirical method uses the reports of damages from past tsunami events to estimate the impact force of the tsunami wave. The analytical method has limitations because the dynamic nature of a tsunami wave cannot be estimated. The numerical method simulates the evolution of the tsunami waves from their point of origin to the impact on the structure but the more detailed and sophisticated the method is, the more computationally expensive it is. However, the advance in computational power of modern hardware makes this method affordable.

These days, mesh based finite element method is used to simulate the tsunami wave propagation. However this method cannot directly compute the impact force exerted from the tsunami wave. An equivalent static impact force must be estimated based on the inundation depth and the velocity of the wave (Palermo, Nistor *et al.* 2009). The force is classified into five components: hydrostatic force, buoyant force, hydrodynamic force, surge force, and debris impact force (Yeh 2007). Based on their occurrence, the different components are classified as: initial impact and post impact. The initial impact is the condition when the tsunami wave advances toward the structure. Surge force and debris impact force happen at this time. Post impact is the condition when the tsunami wave fully surrounds the structure. Hydrodynamic forces, hydrostatic forces, and buoyant forces happen at this time.

2.2.1 Hydrostatic force

The hydrostatic force is generated when the tsunami inundation raises around the structure. The force is caused by the water gradient between inside and outside the structure (Fig. 2(a)). The force acts perpendicular to the plain surface of structure. It may not fully affect a short length structure, because water will overtop the structure and fill in all the empty space, which reduces the water gradient (FEMA 2008). The hydrostatic force is calculated as

$$F_h = p_c \cdot A_w = \frac{1}{2} \rho_s \cdot g \cdot b \cdot h_{\max}^2 \quad (2)$$

where p_c is the hydrostatic pressure, A_w is the wet area of the panel, ρ_s is the fluid density including sediment (1200 kg/m^3), g is the gravity acceleration, b is the width of the wall, and h_{\max} is the maximum water height above the base of the wall at the structure location.

2.2.2 Hydrodynamic force

The hydrodynamic force, also known as drag force, is caused by the friction force of the flowing waves and the pressure force within the flowing mass water (Fig. 2(b)). Hydrodynamic force is generated when the tsunami waves floods the land and the structures with a moderate to high velocity (FEMA 2008). The force is calculated as

$$F_d = \frac{1}{2} \rho_s \cdot C_d \cdot B \cdot (h \cdot u^2)_{\max} \quad (3)$$

where ρ_s is the fluid density including sediment (1200 kg/m³), C_d is the drag coefficient, h is the flow depth, and u is the flow velocity at the location of the structure. B is the width of the component over which the friction is exercised. FEMA recommends that the drag coefficient be taken as $C_d = 2.0$.

2.2.3 Buoyant force

The buoyant force is the hydrostatic forces acting in the vertical direction through the center of mass of the structure when the tsunami wave partially or totally surrounds the structure (Fig. 2(c)). Buoyant force is considered as the weight of tsunami water displaced (FEMA 2008). The light frame buildings, like wood frame, that are built near the coastline should be of concern about buoyant forces due to its small resistance to the upward force. Buoyant force is calculated as:

$$F_b = \rho_s \cdot g \cdot V \quad (4)$$

where ρ_s is the sea water density including sediment (1200 kg/m³), and V is the volume of water displaced by the building (Fig. 2(c)).

2.2.4 Surge force

The surge force also known as impulsive force is caused by the impact of the tsunami wave on the structure. The first tsunami wave that arrives on the coastline will not have a significant surge force but the subsequent tsunami waves that flood the coastline will have (Ramsden 1996, Árnason 2005, Yeh 2007). Surge force affects only the edge of the structure that faces the tsunami waves (FEMA 2008) (Fig. 2(d)). Surge force is calculated as

$$F_s = 1.5F_d \quad (5)$$

where F_d is hydrodynamic force of tsunami wave

2.2.5 Debris impact force

A tsunami wave flooding the land can carry debris of floating pieces of structures, floating cars, drift woods, even ships. The impact of floating debris can reduce the strength of the structures (FEMA 2008). The debris impact force is calculated as

$$F_i = C_m \cdot u_{\max} \cdot \sqrt{k \cdot m} \quad (6)$$

where C_m is the added mass coefficient, u_{\max} is the maximum flow velocity carrying the debris at the site, and m and k are the mass and the effective stiffness of the debris. It is recommended that the added mass coefficient be taken as $C_m = 2.0$.

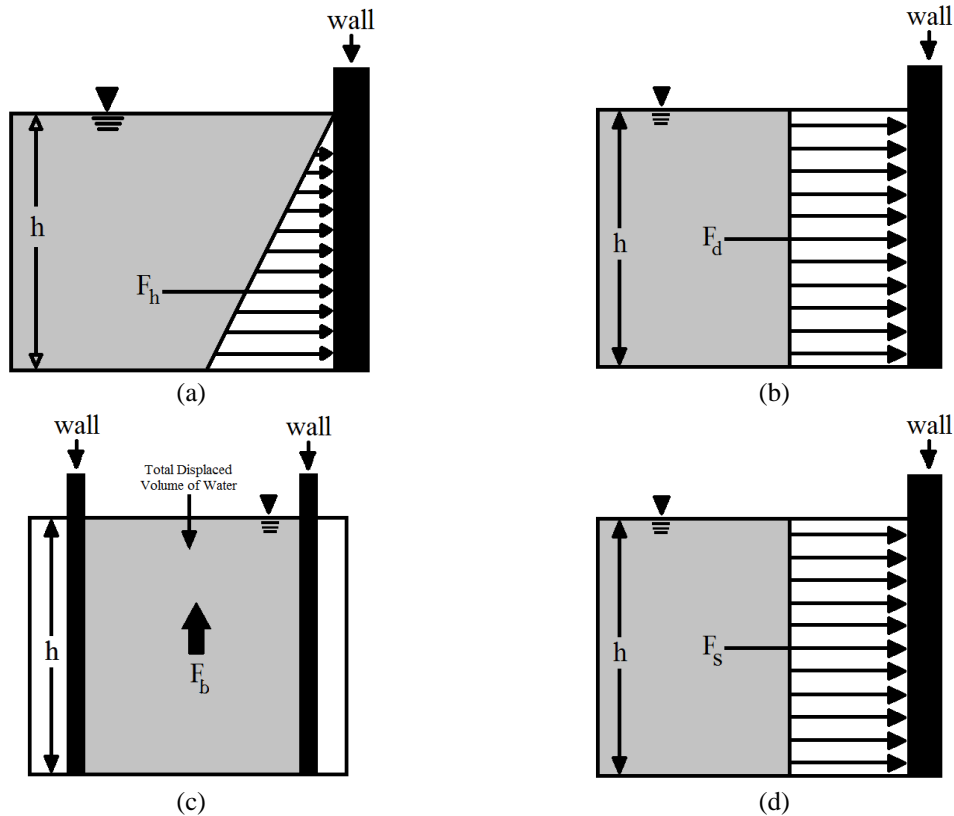


Fig. 2 Static forces distribution and location of resultant: (a) hydrostatic, (b) hydrodynamics, (c) buoyant and (d) surge

2.3 Tsunami simulation using smooth particle hydrodynamics method

Numerical simulation of tsunami waves is a challenge because of its dynamic nature of force evolution, the wave-surface interaction, and the many parameters involved on the boundary conditions and initial conditions. Mesh-based finite element method has difficulties to estimate the tsunami waves impact forces. Most mesh-based finite element method for tsunami simulation are used to estimate the velocity, height, and travel time of tsunami from its source to the coastline, for example: Tsunami (Goto, Ogawa *et al.* 1997), MOST (Titov and Gonzalez 1997). The main benefit of numerical tsunami simulation is the ability to simulate the incoming wave from the source to the coastline. This provides time for the evacuation and minimizes the loss of lives. If also the impact force on the structures could be computed directly for the numerical simulation is more accurate results could be obtained for both prediction and mitigation purposes.

The loading features of the tsunami waves can be estimated by hand employing available formula from previous studied done by many researcher (Yeh 2007). However, the dynamic characteristic of tsunami waves requires a more detailed load estimation method. Numerical tsunami simulation using mesh less methods solves this problem. SPH is a mesh-less numerical

method used in computational fluid dynamics. Its capability to simulate dynamic interaction between fluid and solid object accurately and reliably was proven beneficial for tsunami simulation (Altomare, Crespo *et al.* 2015). However, the computational cost of using SPH method hindered its use up to now. With the advent of general purpose graphic processing unit (GPGPU) in the computational hardware the computational cost of this numerical method was reduce and it is now affordable. A desktop computer or a workstation can run a simulation that was limited to CPU cluster. In this study, DualSPHysics (Crespo, Domínguez *et al.* 2015) is the numerical solver used.

DualSPHysics is one of the developed software based on SPH method. (Gingold and Monaghan 1977) developed the numerical method to solve problems related with astrophysics and cosmology. The numerical problems were solved using meshless methods which is different from the mesh based method (i.e., finite element method). The meshless method provides better benefit than mesh based when it is used to simulate complex geometries problem, when there is a large deformation problem, or when material singularities are involved (Barreiro, Crespo *et al.* 2013). SPH gained popularity because it can track: the density, the pressure, and the velocity of the particles during the simulation. In addition, it can simulate flow even where two surface with different phase are present, i.e. fluid-solid interaction (Barreiro, Crespo *et al.* 2013).

In the beginning, a collaboration of researchers from USA, Spain, and United Kingdom developed SPHysics with intention to solve free-surface flows problem (Gomez-Gesteira, Rogers *et al.* 2012). Examples of free-surface flow problems are: a flood event, a coastline wave break, a wave propagations, a wave loading on structure, a tsunami wave impact. Though SPHysics offers many benefit to estimate particle movement in a mesh-less environment, its major drawback is the computation cost, which requires a lot of resources (Barreiro, Rogers *et al.* 2013). The development of SPHysics on the GPGPU environment resulted in DualSPHysics.

Altomare, Crespo *et al.* (2015) studied the capability of DualSPHysics to estimate the sea wave force on coastal defenses. The study consists of two phases. In the initial phase, validation phase, there are three types of impacts that set for the simulation: standing wave on impermeable fully reflective vertical wall, non-breaking waves on vertical structures, and impulsive provoked breaking waves. The second phase is the application to a real-life problem. The study case are Zeebrugge Harbor and Blankenberge Marina located in Belgium. DualSPHysics was used to estimate the wave forces on the coastal structures. The current limitation of DualSPHysics (i.e., simulate the re-reflected wave) does not hinder its function as an alternative assessment tool that provide reliable data compared with the physical model.

Barreiro, Crespo *et al.* (2013) performed several numerical simulation of wave-structure interaction using DualSPHysics. The validation were done by comparing the numerical result with analytical solution and also with the available experimental data. The two parameter that were observed are the force due to wave breaking and the force due to wave propagation. Following the validation simulation, DualSPHysics is then applied to real-life environment simulation. The scenario is to simulate both the wave propagation and breaking wave at the same time. The wave propagates approaching the coastline and it breaks upon reaching it, the force exerted on the urban landscape and furniture due to impacting wave were observed. DualSPHysics also provides result of the moment that shows the intensity of impact and its distribution point. This is a very useful feature to understand how the interaction between wave and structure during the wave breaking.

Dao, Xu *et al.* (2013) observed the impact on a vertical wall of: non-breaking waves run-up and the breaking solitary waves run-up. The waves are equivalent to a long wave of a tsunami or of a storm. The observation was done by comparing the experimental data with the numerical

simulation produced using DualSPHysics and Tunami-N2. The observation put emphasis on the mechanism of wave run-up (i.e., wave propagation, wave breaking, wave impact on the structure, and the post impact wave run-down) and the pressure exerted by the wave impacting the wall. The comparison between the simulation results and the experimental observations of the wave propagation shows the capability of DualSPHysics to simulate the different possible scenarios.

St-Germain, Nistor *et al.* (2012) investigated the development of the hydrodynamic forces due to the propagation of tsunami wave using SPH method. Two different initial conditions of the sea bed were used: dry bed and wet bed. The results of the numerical simulation were compared to experimental observation. The comparison between the numerical simulation and experimental observation shows good agreement and it demonstrates the capability of the SPH method to simulate the force evolution given different initial bed condition.

The SPH estimation method is based on the integral interpolants, where the function of F is estimated by the approximation

$$F(\mathbf{r}) = \int F(\mathbf{r}')W(\mathbf{r}-\mathbf{r}',h) d\mathbf{r}' \quad (7)$$

where W is the kernel function, r is the particle position, and h is the smoothing length. The kernel function estimates the values of such particle based on the conservation laws of continuum fluid dynamics and smoothing length define the inter-particle distance accounted for particle approximation. The choice of smoothing kernel define the efficiency of SPH estimations, thus smoothing kernel should have positive value along the defined distance, compact support, normalization, and decreasing value as the distance getting far from the source point. In this study, Wendland quintic kernel is employed to define the smoothing kernel. The Wendland kernel is defined as

$$W(q) = \alpha_D \left(1 - \frac{q}{2}\right)^4 (2q+1), \quad 0 \leq q \leq 2 \quad (8)$$

where q is the non-dimensional distance between particles, and α_D is the normalization constant in three dimension space state.

The particle acceleration in SPH method is defined as

$$\frac{dv_a}{dt} = -\sum m_b \left(\frac{P_b}{\rho_b^2} + \frac{P_a}{\rho_a^2} + \Pi_{ab} \right) \nabla_a W_{ab} + g \quad (9)$$

where v is velocity, P is pressure, ρ is density, m is mass, g is gravitational acceleration, W_{ab} is the kernel function between particle a and b , Π_{ab} is the viscosity. The pressure of particle is defined as

$$P_a = B \left[\left(\frac{\rho_a}{\rho_0} \right)^\gamma - 1 \right] \quad (10)$$

where ρ is fluid density, and B and γ are constant.

2.3.1 Removal of static force limitation

The scope of this study is to avoid over simplification of surge force. Following the FEMA

method, computing the surge force as 150% of the hydrodynamic forces (Eq. (5)) reduces a highly non-linear forces to a static one. The same concept is present in earthquake engineering when one design a structure using equivalent static analysis instead of non-linear time history analysis.

In this study, the time history of the tsunami wave height is used to compute the time histories for the hydrostatic force, and the buoyant force using the given equations (Eqs. (2) and (4)). Instead, the time histories of drag force and surge force is given directly by the SPH model through integration of the wave pressure over the front surface of the structure.

2.4 Structural model using finite element method

OpenSees (McKenna 2011), is an open source finite element solver developed by Frank McKenna from UC Berkeley. OpenSees is an object-oriented, software framework supported by joint cooperation between Pacific Earthquake Engineering Research Center (PEER) and the George E. Brown Jr. Network for Earthquake Engineering Simulation (NEES), and sponsored by National Science Foundation (NSF). The intention of OpenSees development is to encourage improvement on the nonlinear earthquake engineering research and create an active communities between researchers and practitioners.

In this study, OpenSees is used to compute both the capacity of the structure and the demand of the impact force of the tsunami. The capacity is computed using non-linear static analysis. Moment-curvature analysis to assess the capacity of the reinforced concrete cross-section subject to bending moment and axial force. Push-over analysis to assess the capacity of the columns subject to shear force. The demand is computed using non-linear dynamic analysis. The model includes all possible sources of material non-linearity for: cover concrete and core concrete (Yassin 1994), longitudinal steel rebar (Filippou, Popov *et al.* 1983), and the time history of the impact force, which is recorded in the SPH simulation. Detailed information of structural model can be found below.

2.4.1 Prototype of the structural model

The prototype model is a three-story building that is 6 m long, 6 m wide, and 3.6 m high each story. It has 4 reinforced concrete square columns (Fig. 4). In this study we built two models of the structure. The differences are the column cross-section and reinforcing steel content. In Model01 the cross-section is 71.12 x 71.12 cm, adapted from the model example from Opensees (McKenna 2011).

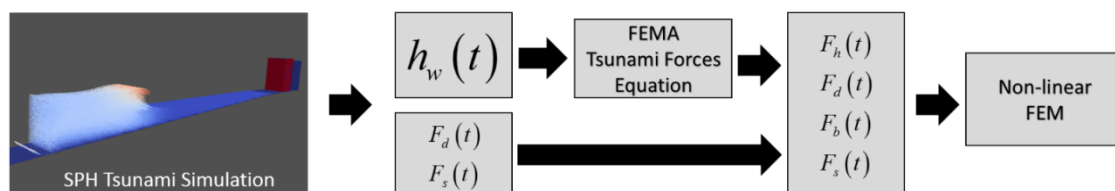


Fig. 3 Estimation of nonlinear tsunami forces using SPH method

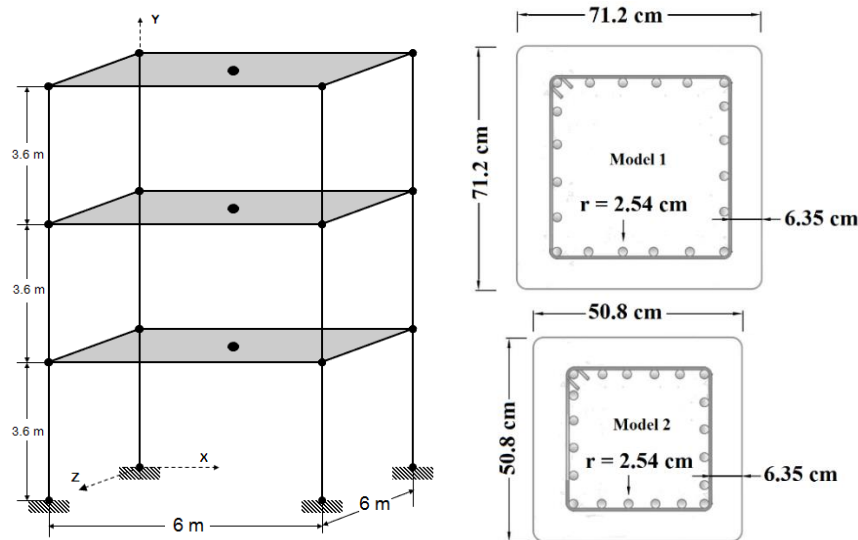


Fig. 4 Geometry of structural model and its column cross section

In Model02 the cross-section is remodeled to 50.8 x 50.8 cm. The cross-section of the beam is 60.9 x 45.7 cm for both model. Columns have 20 longitudinal rebars with a radius of 2.54 cm the yielding stress (σ_y) is 460 MPa.

To model the behavior of column a fiber section was used. The core inside the rebars was modeled with confined concrete, the cover was modeled with unconfined concrete. The elastic modulus of the concrete is $E_s = 24.85$ GPa. The equivalent compressive strength of the confined concrete is $\sigma_{cc} = 35.85$ MPa and the compressive strength of the unconfined concrete is $\sigma_{cu} = 27.5$ MPa. The non-linear behavior of the structure is modeled using “nonlinearBeam” elements (Taucer, Spacone *et al.* 1991, Spacone *et al.* 1992, Neuenhofer and Filippou 1997), “fiber” sections, and non-linear uniaxial behavior models of the materials: core concrete, cover concrete, longitudinal steel rebars. The uniaxial stress-strain (σ - ϵ) relationship of the concrete uses “Concrete02” (Yassin 1994). Different behavior in the non-linear range is adopted for core concrete, i.e., confined, and cover concrete, i.e., unconfined. The uniaxial stress-strain relationship of the longitudinal steel rebars uses “Steel02” based on Giuffre-Menegotto steel material object with isotropic hardening (Filippou, Popov *et al.* 1983).

2.5 Damage states of structure

The damage caused by tsunami impact on structures can be varying from no damage to collapse, followed 2011 Tohoku tsunami this topic has been observed extensively by. In this study, the damage occurred on structure is assessed from ductility demand. Due to impact of uplift buoyant force and lateral tsunami forces (hydrostatics, hydrodynamics and surge force) the column lose its strength and stiffness in the inelastic condition. The ductility demand of column structure estimated from chord rotation considered as good estimation to define the damage state (Kim and Feng 2003).

Table 1 Damaged states of column

Damage state	Description	Ductility demand
No damage	First yield	1
Minor damage	Cracking, spalling	1.7
Moderate damage	Loss of anchorage	2.4
Major damage	Incipient column collapse	3.2
Collapse	Column collapse	7

The damage states in this research are defined into five states: 1) no damage, 2) minor damage, 3) moderate damage, 4) major damage, 5) collapse where the structure impacted from the exerted forces of tsunami wave. For every damage states, the ductility demand are adapted from the MCEER research on fragility curve of column in USA as found in Dutta and Mander (2001). These ductility demands estimated from the drift limits of every damage states.

2.6 Computation of fragility curves

The capacity of structures to withstand the impact of disasters, such as: ground motion from an earthquake, tsunami waves impact, typhoon impact, is represented by fragility curves. The fragility curves are cumulative distribution functions that express the probability of failure of a structure as a function of an intensity measure of tsunami hazard. Lognormal distribution functions are used and the maximum likelihood method is used to estimate the parameters of the functions: median and log-standard deviation, (Shinozuka, Feng *et al.* 2000, Kim and Feng 2003, Koshimura, Namegaya *et al.* 2009, Torbol, Gomez *et al.* 2013). In this research, the intensity measure used to represent the tsunami waves are: maximum wave height at the coastline and maximum wave height at the time of impact on the structure. The damage states are obtained by comparing the capacity of the structure: the ductility and the structure displacement with the demand of the tsunami waves. The cumulative probability P_j of occurrence of the damage state j is given by

$$P_j = F(X) = \Phi \left[\frac{\ln X - c_m}{\zeta} \right] \quad (11)$$

where Φ is the standard normal distribution, X is the intensity measure taken into consideration, c_m and ζ are the mean and standard deviation of lognormal X .

In this study, we follow the second method of fragility curve estimation framework of Torbol, Gomez *et al.* (2013) and Shinozuka, Feng *et al.* (2000). The maximum likelihood method is used to compute the median and log-normal standard deviation. The parameters of fragility curves of each damage state estimated concurrently. The fragility curves of respective damage state in this method have the same log-normal standard deviation. Because of it they are parallel on a lognormal probability paper and for any value of the intensity measure the correct order of progressive damage is guaranteed: minor, moderate, major, collapse is respected. (Shinozuka, Feng *et al.* 2000).

The likelihood function that has to be maximized is

$$L = \prod_{i=1}^N [F(h_{w,i})]^{x_i} [1 - F(h_{w,i})]^{1-x_i} \quad (12)$$

where $F(h_{w,i})$ represent the fragility curve of the specific damage state, in this study there four damage states (i.e., at least minor, at least moderate, at least major, collapse), $h_{w,i}$ is the wave height at the point of observation of the simulation i , x_i is the realization of the Bernoulli random variable of $h_{w,i}$. $x_i=1$ if the simulation i causes the structure above the damage state and $x_i=0$ if the simulation i does not cause the structure above the damage state. N is the total number of tsunami waves simulations in the data set.

Each damage state is assigned one exclusive event: E_0 no damage, E_1 minor, E_2 moderate, E_3 major, E_4 collapse. $P_j=P(X,E_j)$ is the probability of structure at the intensity measure X for damage state E_j . The analytical form to estimate the fragility curves is expressed as

$$F_j(X_i; c_{m,j}; \zeta_j) = \Phi \left[\frac{\ln(X_i / c_{m,j})}{\zeta_j} \right] \quad (13)$$

where $c_{m,j}$ and ζ_j are the single value median and log-standard deviation of the fragility curves applied for every assigned damage state (i.e., at least minor, at least moderate, at least major, collapse) that is identified by the j indices = 0, 1, 2, 3 and 4 respectively. The probability of each damage states can be obtained by the following expressions

$$P_{i,0} = P(a_i, E_0) = 1 - F_1(a_i; c_{m,1}, \zeta) \quad (14)$$

$$P_{i,1} = P(a_i, E_1) = F_1(a_i; c_{m,1}, \zeta) - F_2(a_i; c_{m,2}, \zeta) \quad (15)$$

$$P_{i,2} = P(a_i, E_2) = F_2(a_i; c_{m,2}, \zeta) - F_3(a_i; c_{m,3}, \zeta) \quad (16)$$

$$P_{i,3} = P(a_i, E_3) = F_3(a_i; c_{m,3}, \zeta) - F_4(a_i; c_{m,4}, \zeta) \quad (17)$$

$$P_{i,4} = P(a_i, E_4) = F_4(a_i; c_{m,4}, \zeta) \quad (18)$$

The likelihood function for the damage stage can be written as

$$L(c_1, c_2, c_3, c_4, \zeta) = \prod_{i=1}^N \prod_{k=0}^4 P_k(a_i; E_k)^{x_{ik}} \quad (19)$$

where $x_{ik}=1$ if there is a damage within E_k state occurs in the structural model due to tsunami wave height = a_i and $x_{ik}=0$ if otherwise.

3. Results

The tsunami simulations were performed using DualSPHysics. Each simulation has its own height of tsunami waves at the coastline and at the point of impact on the structure. The structural response due to forces exerted from the tsunami wave on the structure was computed using the OpenSees, the capacity of the structure is also computed using OpenSees. The damage states of the structure were determined from the moment curvature analysis of the cross-section of the columns and its ductility. The damage states are: minor damage, moderate damage, major damage and collapse. For the structural model in this study we have two structural models. The first model, Model01, is adapted from Opensees examples for 3D structural modeling & analysis. The second model, Model02, is modified from the first model with smaller column dimension. The column width for Model01 and Model 02 are 71.2 cm and 50.8 cm respectively. In this study we define: moving boundary conditions for the wave maker section, close boundary condition for the lateral borders, and open channel boundary condition for the coastline end section. The open channel boundary condition simulates the flow of tsunami wave, flooding the dry land until its end process. Therefore, once the wave passed the structure there will be no wave reflection that might affect the structure and our estimation of fragility curve.

3.1 Numerical model of tsunami simulation

The computational domain for the tsunami wave simulation was setup with closed boundaries. The domain included 176,849 particles. The total time step used in this study is 200 time steps with distance between particles is 0.25 m and the smoothing length is 0.866 m. The distance between particle only affect the accuracy of the computed force to a certain degree. If the distance is too large it will impact the accuracy of force calculation over an area, however if the distance is too small it needs more computational power than the single GPU RAM can handle. In this study, the distance between particles is decided as the better trade off after our previous trial runs. A simple coastline was designed and the base of the domain with a gradient height difference. The difference between coastline and the base is 5 m and the length is 90 m, which create an angle $\theta = 3.18^\circ$ between the water surface and the coastline. The model of the structure was located 10 m away from the coastline. At $t = 0$, the water is in stationary position. At $t > 0$, the wave-maker starts to move pushing the water toward coastline to generate the first tsunami wave and then it move away from the coastline to generate the second tsunami wave. In the different simulations the wave maker moves forward and backward with a different combination of properties, such as speed, and it generates the different tsunami waves breaking at the coastline. During the simulation the height of the waves and the load on the structures are recorded. The height is recorded in two different places: at the coastline and at the structural model (Fig. 5).

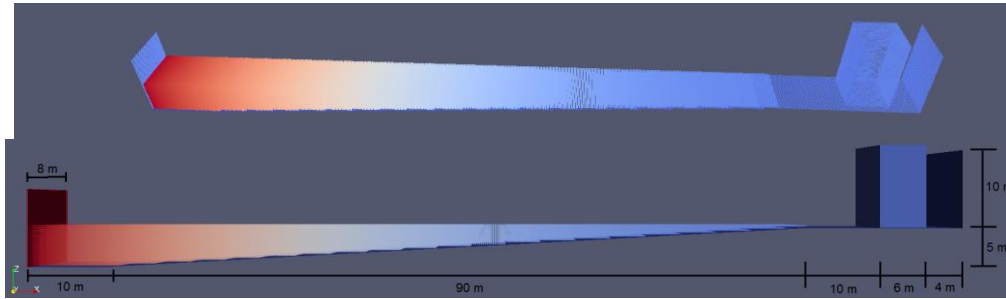


Fig. 5 Configuration of tsunami wave model and building model

3.2 Data set of tsunami waves

A total of 96 tsunami simulation were performed on the DualSPHysics. Fig. 6 shows how the tsunami wave arrives at the coastline and how it hits the structure. The maximum tsunami wave heights at the coastline and at the structure are shown in Table 2. The hydrodynamics and surge force exerted on the structure, which are also obtained directly from DualSPHysics, are shown in Fig. 7. The evolution of the wave height over time are shown in Fig. 8. The wave height evolution was used to calculate the other forces: hydrostatics, and buoyant force

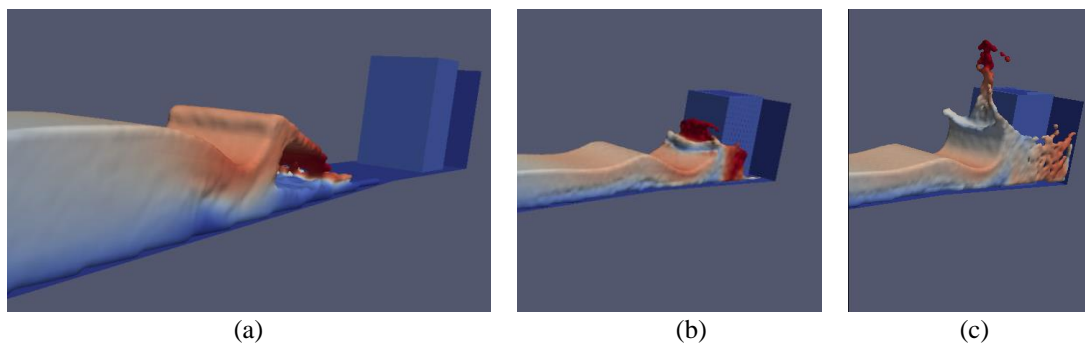


Fig. 6 Side view of tsunami wave simulated on DualSPHysics (a) arriving at coast line and approaching the structural model, (b) and (c) impacting the structural model

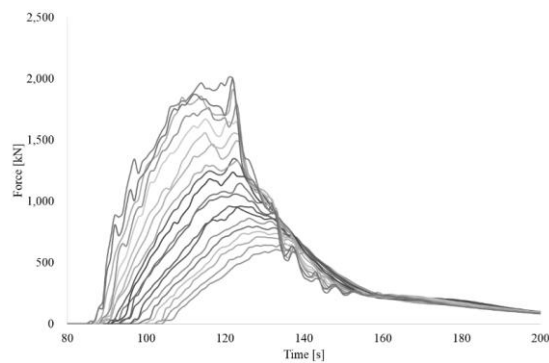


Fig. 7 Exerted hydrodynamic forces on structure recorded from DualSPHysics simulations

Table 2 Maximum wave height recorded from simulations using DualSPHysics

Simulation ID	Max height at the coastline	Max height at the coastline	Simulation ID	Max height at the coastline	Max height at the coastline	Simulation ID	Max height at the coastline	Max height at the coastline
Sim_001	5.445 m	9.715 m	Sim_033	5.485 m	8.485 m	Sim_065	6.235 m	12.755 m
Sim_002	5.355 m	10.105 m	Sim_034	5.235 m	8.055 m	Sim_066	5.885 m	12.335m
Sim_003	5.815 m	10.385 m	Sim_035	4.635 m	7.745 m	Sim_067	3.265 m	5.785 m
Sim_004	5.635 m	10.565 m	Sim_036	4.495 m	7.425 m	Sim_068	3.375 m	5.755 m
Sim_005	5.795 m	10.775m	Sim_037	4.315 m	7.235 m	Sim_069	3.455 m	6.255 m
Sim_006	6.175 m	11.175 m	Sim_038	4.075 m	6.955 m	Sim_070	3.555 m	6.385 m
Sim_007	5.935 m	12.695 m	Sim_039	4.045 m	6.565 m	Sim_071	3.635 m	6.645 m
Sim_008	5.815 m	11.925 m	Sim_040	3.835 m	6.455 m	Sim_072	3.685 m	7.025 m
Sim_009	5.465 m	13.115 m	Sim_041	3.763 m	6.015 m	Sim_073	3.875 m	7.265 m
Sim_010	5.525 m	12.655 m	Sim_042	3.635 m	5.785 m	Sim_074	4.095 m	7.655m
Sim_011	5.665 m	14.675 m	Sim_043	3.495 m	5.555 m	Sim_075	4.045 m	7.775 m
Sim_012	6.205 m	14.990 m	Sim_044	3.455 m	5.235 m	Sim_076	4.275 m	8.205m
Sim_013	6.925 m	14.915 m	Sim_045	3.305 m	4.925 m	Sim_077	4.475m	8.565 m
Sim_014	6.905 m	13.935 m	Sim_046	3.215 m	4.725 m	Sim_078	4.445 m	8.715 m
Sim_015	7.235 m	14.555 m	Sim_047	4.665 m	7.325 m	Sim_079	4.525 m	9.345 m
Sim_016	7.865 m	14.265 m	Sim_048	4.785 m	7.565 m	Sim_080	4.645 m	9.355m
Sim_017	8.075 m	13.465 m	Sim_049	5.195 m	7.915 m	Sim_081	4.725 m	9.745 m
Sim_018	8.005 m	12.595 m	Sim_050	5.245 m	8.165 m	Sim_082	4.815 m	9.895 m
Sim_019	8.465 m	12.965 m	Sim_051	5.495 m	8.415m	Sim_083	4.895 m	10.465m
Sim_020	8.835 m	13.305 m	Sim_052	5.655 m	8.595 m	Sim_084	4.865 m	11.355 m
Sim_021	9.115 m	14.990 m	Sim_053	6.045 m	8.975m	Sim_085	4.845 m	11.965 m
Sim_022	9.355 m	14.990 m	Sim_054	5.905 m	9.185 m	Sim_086	4.815 m	13.645 m
Sim_023	9.735 m	14.990 m	Sim_055	6.595 m	9.575 m	Sim_087	4.885 m	11.735 m
Sim_024	9.275 m	14.990 m	Sim_056	6.375m	9.915 m	Sim_088	5.045 m	13.445 m
Sim_025	9.795 m	14.990 m	Sim_057	6.625 m	10.345 m	Sim_089	5.185 m	13.675m
Sim_026	9.545 m	14.990 m	Sim_058	6.255 m	10.595 m	Sim_090	5.445 m	14.535 m
Sim_027	9.475 m	14.990 m	Sim_059	6.475 m	10.795 m	Sim_091	5.445 m	13.405 m
Sim_028	9.955 m	14.990 m	Sim_060	6.625 m	10.955 m	Sim_092	5.815 m	14.065m
Sim_029	8.375 m	14.990 m	Sim_061	7.015 m	11.235 m	Sim_093	6.195 m	13.735 m
Sim_030	7.645 m	14.990 m	Sim_062	6.665 m	12.275 m	Sim_094	6.185 m	13.965 m
Sim_031	5.865 m	9.055m	Sim_063	6.325 m	12.725 m	Sim_095	6.675 m	14.205 m
Sim_032	5.705 m	8.685 m	Sim_064	6.725 m	12.935 m	Sim_096	7.545 m	12.605 m

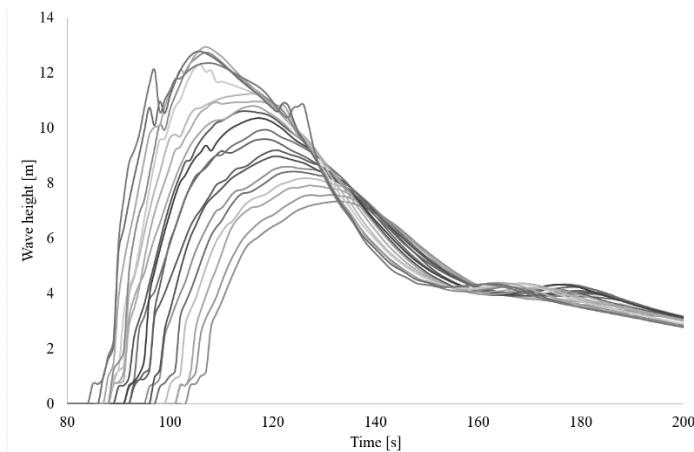


Fig. 8 Ex Tsunami wave height fluctuation, inundated structural model recorded from DualSPHysics simulations

3.3 Capacity of the Structure

Moment-curvature analysis is used to assess the progressive ductility, curvature, and bending moment of the cross-section of the column (Fig. 9). Ductility is defined as the ratio between the deformation of the structure when a force is applied and the deformation of the structure at the yield stage (Priestley 1996). Ductility is calculated as

$$\mu_{\varphi} = \frac{\varphi_u}{\varphi_y} \quad (20)$$

where φ_u is the ultimate curvature and φ_y is the yield curvature. The member ductility capacity of column in this study is 7.0.

3.4 Structural response to tsunami impact

The structural responses were computed with OpenSees using non-linear dynamic analysis. The number of steps and the size of the step is the same in OpenSees and DualSPHysics, $T = 200$ steps. This allows the direct application of the impact force recorded in DualSPHysics to the OpenSees model. The damages due to the impact of the tsunami waves was computed by comparing capacity and demand and the results are shown in Tables 3 and 4.

Table 3 Damage State of the structural model 01 due to tsunami wave impact

Simulation ID	Damage State						
Sim_001	No Damage	Sim_025	No Damage	Sim_049	No Damage	Sim_073	No Damage
Sim_002	No Damage	Sim_026	Minor	Sim_050	No Damage	Sim_074	No Damage
Sim_003	No Damage	Sim_027	Minor	Sim_051	No Damage	Sim_075	No Damage
Sim_004	No Damage	Sim_028	Moderate	Sim_052	No Damage	Sim_076	No Damage
Sim_005	No Damage	Sim_029	Major	Sim_053	No Damage	Sim_077	No Damage
Sim_006	No Damage	Sim_030	Collapse	Sim_054	No Damage	Sim_078	No Damage
Sim_007	No Damage	Sim_031	No Damage	Sim_055	No Damage	Sim_079	No Damage
Sim_008	No Damage	Sim_032	No Damage	Sim_056	No Damage	Sim_080	No Damage
Sim_009	No Damage	Sim_033	No Damage	Sim_057	No Damage	Sim_081	No Damage
Sim_010	No Damage	Sim_034	No Damage	Sim_058	No Damage	Sim_082	No Damage
Sim_011	No Damage	Sim_035	No Damage	Sim_059	No Damage	Sim_083	No Damage
Sim_012	No Damage	Sim_036	No Damage	Sim_060	No Damage	Sim_084	No Damage
Sim_013	No Damage	Sim_037	No Damage	Sim_061	No Damage	Sim_085	No Damage
Sim_014	No Damage	Sim_038	No Damage	Sim_062	No Damage	Sim_086	No Damage
Sim_015	No Damage	Sim_039	No Damage	Sim_063	No Damage	Sim_087	No Damage
Sim_016	No Damage	Sim_040	No Damage	Sim_064	No Damage	Sim_088	No Damage
Sim_017	No Damage	Sim_041	No Damage	Sim_065	No Damage	Sim_089	No Damage
Sim_018	No Damage	Sim_042	No Damage	Sim_066	No Damage	Sim_090	No Damage
Sim_019	No Damage	Sim_043	No Damage	Sim_067	No Damage	Sim_091	No Damage
Sim_020	No Damage	Sim_044	No Damage	Sim_068	No Damage	Sim_092	No Damage
Sim_021	No Damage	Sim_045	No Damage	Sim_069	No Damage	Sim_093	No Damage
Sim_022	No Damage	Sim_046	No Damage	Sim_070	No Damage	Sim_094	No Damage
Sim_023	No Damage	Sim_047	No Damage	Sim_071	No Damage	Sim_095	No Damage
Sim_024	Minor	Sim_048	No Damage	Sim_072	No Damage	Sim_096	No Damage

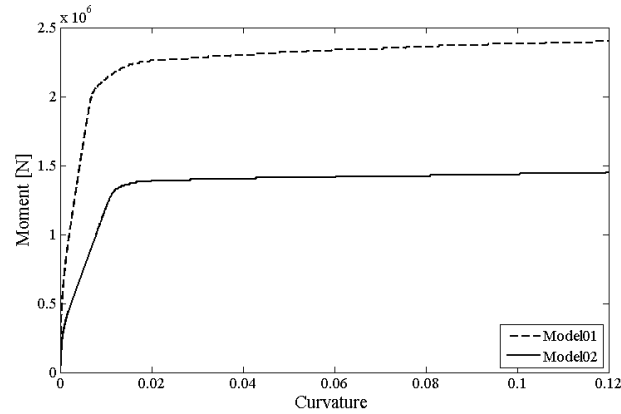


Fig. 9 Moment curvatures analysis of the column of the structural model used in this research

3.5 Fragility curves results

The fragility curves are plotted Fig. 10 to 13 and the parameters are shown in Table 5.

Table 4 Damage State of the structural model 02 due to tsunami wave impact

Simulation ID	Damage State						
Sim_001	No Damage	Sim_025	Collapse	Sim_049	No Damage	Sim_073	No Damage
Sim_002	No Damage	Sim_026	Collapse	Sim_050	No Damage	Sim_074	No Damage
Sim_003	No Damage	Sim_027	Collapse	Sim_051	No Damage	Sim_075	No Damage
Sim_004	No Damage	Sim_028	Collapse	Sim_052	No Damage	Sim_076	No Damage
Sim_005	No Damage	Sim_029	Collapse	Sim_053	No Damage	Sim_077	No Damage
Sim_006	No Damage	Sim_030	Collapse	Sim_054	No Damage	Sim_078	No Damage
Sim_007	No Damage	Sim_031	No Damage	Sim_055	No Damage	Sim_079	No Damage
Sim_008	No Damage	Sim_032	No Damage	Sim_056	No Damage	Sim_080	No Damage
Sim_009	Minor	Sim_033	No Damage	Sim_057	No Damage	Sim_081	No Damage
Sim_010	Minor	Sim_034	No Damage	Sim_058	No Damage	Sim_082	No Damage
Sim_011	Major	Sim_035	No Damage	Sim_059	No Damage	Sim_083	No Damage
Sim_012	Collapse	Sim_036	No Damage	Sim_060	No Damage	Sim_084	No Damage
Sim_013	Collapse	Sim_037	No Damage	Sim_061	No Damage	Sim_085	No Damage
Sim_014	Collapse	Sim_038	No Damage	Sim_062	Minor	Sim_086	No Damage
Sim_015	Collapse	Sim_039	No Damage	Sim_063	Moderate	Sim_087	No Damage
Sim_016	Collapse	Sim_040	No Damage	Sim_064	Moderate	Sim_088	Minor
Sim_017	Collapse	Sim_041	No Damage	Sim_065	Minor	Sim_089	Minor
Sim_018	Collapse	Sim_042	No Damage	Sim_066	Major	Sim_090	Minor
Sim_019	Collapse	Sim_043	No Damage	Sim_067	No Damage	Sim_091	Minor
Sim_020	Collapse	Sim_044	No Damage	Sim_068	No Damage	Sim_092	Minor
Sim_021	Collapse	Sim_045	No Damage	Sim_069	No Damage	Sim_093	Minor
Sim_022	Collapse	Sim_046	No Damage	Sim_070	No Damage	Sim_094	Minor
Sim_023	Collapse	Sim_047	No Damage	Sim_071	No Damage	Sim_095	Minor
Sim_024	Collapse	Sim_048	No Damage	Sim_072	No Damage	Sim_096	Minor

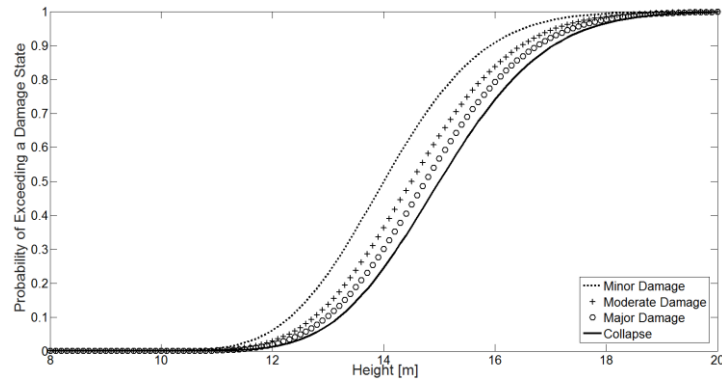


Fig. 10 Fragility curves of Model01 function of the wave height at the structure

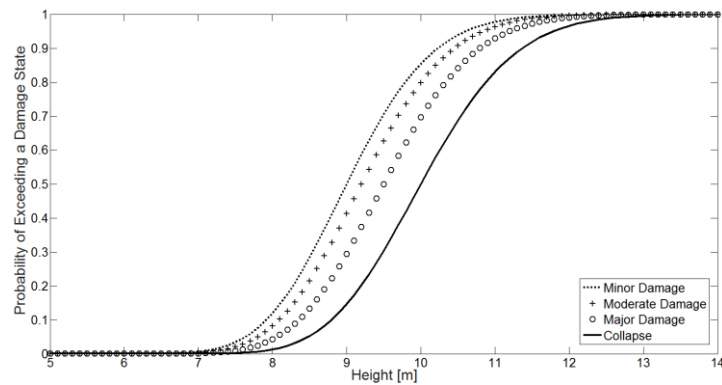


Fig. 11 Fragility curves of Model01 function of the wave height at the coastline

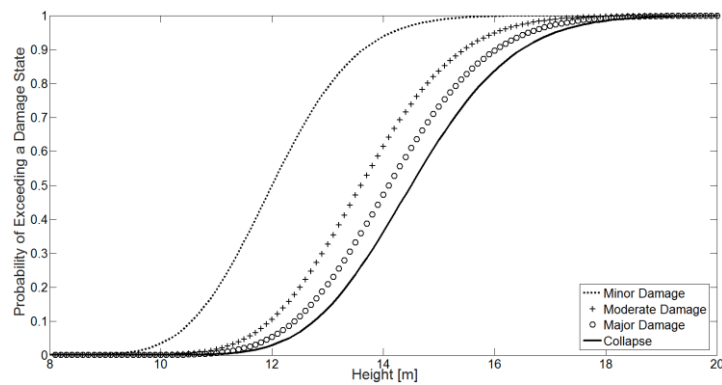


Fig. 12 Fragility curves of Model02 function of the wave height at the structure

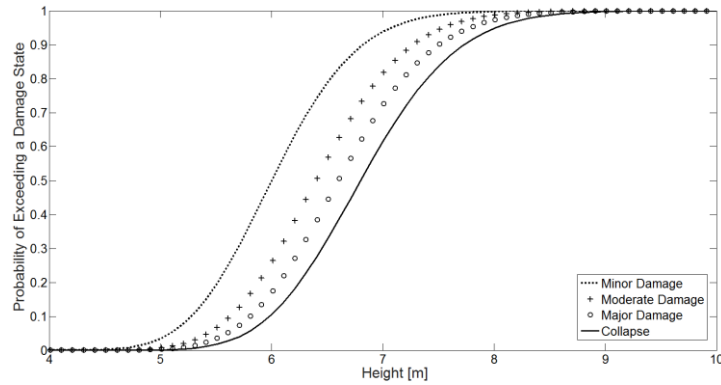


Fig. 13 Fragility curves of Model02 function of the wave height at the coastline

Table 5 Fragility parameters of fragility curves

Structure	Reference wave height	Damage state	Median (c_m)	Sid (ζ)
Model 1	Height at the structure	minor	14.00	0.10
		moderate	14.50	
		major	14.75	
		collapse	15.00	
Model 1	Height at the coastline	minor	9.00	0.10
		moderate	9.20	
		major	9.50	
		collapse	10.00	
Model 2	Height at the structure	minor	12.00	0.10
		moderate	13.60	
		major	14.10	
		collapse	14.50	
Model 2	Height at the coastline	minor	6.00	0.10
		moderate	6.40	
		major	6.60	
		collapse	6.80	

4. Conclusions

Study demonstrates that it is possible to assess the condition of a structure subject to tsunami waves using non-linear dynamic analysis at every stage of the computation. Nowadays, smooth particle hydrodynamics (SPH) method is affordable because of GPGPU computing and it can be used to compute the evolution of dynamic forces on the target structure. The computation of the dynamic forces through a simple linear equation function of the tsunami height should be avoided because the fluid structure interaction is a nonlinear phenomenon. While the hydrostatic force and buoyant force can be computed from the time history of the wave height at the structure, the drag and the surge force should be retrieved from the tsunami simulation.

SPH method is used over mesh-based method because it can compute the pressure on any surfaces and at any boundaries of the model including buildings. This study shows how SPH can be used to propagate a tsunami wave inland and how it can be coupled with the FEM model of a structure to compute fragility curves. The entire framework follows the same path used to compute fragility curves of building subject to earthquake. However, while the time history of a ground motion is the only necessary and sufficient input to the non-linear time history analysis of the structure, the time history of the tsunami wave height is not sufficient. The forces due to earthquake within a structure are only function of the ground motion acceleration and mass of the structure. Instead, the forces due to tsunami within a structure are function of the structure geometry and its interaction with the tsunami wave, i.e. fluid structure interaction. This requires large scale SPH simulation.

The intensity measure used in this study is another issue because there is no well established intensity measure for tsunami risk assessment. We proposed and used: the height at the coastline because it is a parameter common to all the structures in the same area, and the maximum height at the structure. Other intensity measures can be investigated but the amplitude, the shape, and the duration of tsunami waves varies widely between the different cases.

The results show that Model01, which has the biggest cross section of the columns and the highest confinement ratio, withstands a tsunami wave better than Model02. However, once its columns enter the plastic range it can withstand little additional hydrodynamic force. A tsunami wave generates a monotonic incremental force on the structure. This force is similar to an impulse ground motion although it builds up slower. The columns have little time to absorb the force through their plastic range. This effect is less pronounced than the one caused by an impulse ground motion. Because the hydrodynamic force is not a function of the mass of the structure increasing the elastic range of the columns rather than increasing their ductility is the best option to withstand a tsunami. Furthermore, from these results it is the researchers' opinion that a structure with rectangular columns or shear walls perpendicular to the coast line will have the highest elastic range to withstand a tsunami without increasing the mass involved, which makes it weaker to ground motion forces. This requires additional future research, simulation, and experiments.

The data set of tsunami simulations was carried out on a single GPU. Our future research focuses on the generation of tsunami waves at their point of origin and their propagation up to the coastline and structures present on it. These SPH models will require the use of billions of particles and multi-GPU systems. However, the analytical fragility curves of this study will be used to assess the status of the structures over the entire area affected by the tsunami waves.

Acknowledgments

This work was supported by the year of 2012-2013 Research Funds of the Ulsan National Institute of Science and Technology (UNIST).

References

- Altomare, C., Crespo, A.J.C., Domínguez, J.M., Gómez-Gesteira, M., Suzuki, T. and Verwaest, T. (2015), "Applicability of smoothed particle hydrodynamics for estimation of sea wave impact on coastal structures", *Coast. Eng.*, **96**, 1-12.

- Altomare, C., Crespo, A.J.C., Rogers, B.D., Dominguez, J.M., Gironella, X. and Gómez-Gesteira, M. (2014), "Numerical modelling of armour block sea breakwater with smoothed particle hydrodynamics", *Comput. Struct.*, **130**, 34-45.
- Árnason, H. (2005), Interactions between an Incident Bore and a Free-Standing Coastal Structure, University of Washington, Ph.D Thesis.
- Barreiro, A., Crespo, A.J.C., Domínguez, J.M. and Gómez-Gesteira, M. (2013), "Smoothed particle hydrodynamics for coastal engineering problems", *Comput. Struct.*, **120**, 96-106.
- Borrero, J.C. (2005), "Field data and satellite imagery of Tsunami effects in banda aceh", *Science*, **308**(5728), 1596-1596.
- Crespo, A.J.C., Domínguez, J.M., Rogers, B.D., Gómez-Gesteira, M., Longshaw, S., Canelas, R., Vacondio, R., Barreiro, A. and García-Feal, O. (2015), "Dualsphysics: Open-source parallel Cfd solver based on smoothed particle hydrodynamics (Sph)", *Comput. Phys. Commun.*, **187**, 204-216.
- Dao, M.H., Xu, H., Chan, E.S. and Tkalich, P. (2013), "Modelling of Tsunami-like wave run-up, breaking and impact on a vertical wall by Sph method", *Natural Hazards and Earth System Science*, **13**(12), 3457-3467.
- Dutta, A. and Mander, J. (2001), Rapid and Detailed Seismic Fragility Analysis of Highway Bridges, *Unpublished Technical Report MCEER*.
- FEMA (2008), *Guidelines for Design of Structures for Vertical Evacuation from Tsunamis (Fema P646)*, Federal Emergency Management Agency.
- Filippou, F.C., Popov, E.P. and Bertero, V.V. (1983), Effects of Bond Deterioration on Hysteretic Behavior of Reinforced Concrete Joints.
- Gingold, R.A. and Monaghan, J.J. (1977), "Smoothed particle hydrodynamics: Theory and application to non-spherical stars", *MNRAS*, **181**(3), 375-389.
- Gisler, G., Weaver, R.P. and Gittings, M. (2010), Calculations of Tsunamis from Submarine Landslides, *Submarine Mass Movements and Their Consequences*, Springer, 695-704.
- Gomez-Gesteira, M., Rogers, B.D., Crespo, A.J.C., Dalrymple, R.A., Narayanaswamy, M. and Dominguez, J.M. (2012), "Sphysics – development of a free-surface fluid solver – Part 1: theory and formulations", *Comput. Geosci.*, **48**, 289-299.
- Goto, C., Ogawa, Y., Shuto, N. and Imamura, F. (1997), *Iugg/Ioc Time Project: Numerical Method of Tsunami Simulation with the Leap-Frog Scheme*, Unesco.
- Hill, E.M., Borrero, J.C., Huang, Z., Qiu, Q., Banerjee, P., Natawidjaja, D.H., Elosegui, P., Fritz, H.M., Suwargadi, B.W., Pranantyo, I.R., Li, L., Macpherson, K.A., Skanavis, V., Synolakis, C.E. and Sieh, K. (2012), "The 2010 Mw 7.8 mentawai earthquake: Very shallow source of a rare Tsunami earthquake determined from Tsunami field survey and near-field Gps data", *J. Geophys. Res.*, **117**(6), 1-21.
- Horwitz, C.B., Lovholt, F., Pedersen, G. and Masson, D.G. (2006), "Mechanisms of Tsunami generation by submarine landslides: A short review", *Norsk Geologisk Tidsskrift*, **86**(3), 255-264.
- Joseph, A. (2011), *Tsunamis: Detection, Monitoring, and Early-Warning Technologies*, Academic Press.
- Kim, S.H. and Feng, M.Q. (2003), "Fragility analysis of bridges under ground motion with spatial variation", *Int. J. Nonlinear Mech.*, **38**(5), 705-721.
- Koshimura, S., Namegaya, Y. and Yanagisawa, H. (2009), "Tsunami fragility - a new measure to identify Tsunami damage", *J. Disaster Res.*, **4**(6), 479-488.
- McKenna, F. (2011), "Opensees: A framework for earthquake engineering simulation", *Comput. Sci. Eng.*, **13**(4), 58-66.
- Mohammed, F. and Fritz, H.M. (2010), "Experiments on Tsunamis generated by 3d granular landslides", *Submarine Mass Movements and Their Consequences*, Springer, 705-718.
- Mori, N., Takahashi, T., Yasuda, T. and Yanagisawa, H. (2011), "Survey of 2011 Tohoku earthquake Tsunami inundation and run-up: Survey of 2011 Tohoku earthquake Tsunami", *Geophys. Res. Lett.*, **38**(7), 1-6.
- National Tsunami Warning, C. (2014), Physics of Tsunamis.
- Neuenhofer, A. and Filippou, F.C. (1997), "Evaluation of nonlinear frame finite-element models", *J. Struct. Eng. - ASCE*, **123**(7), 958-966.

- Palermo, D., Nistor, I., Nouri, Y. and Cornett, A. (2009), "Tsunami loading of near-shoreline structures: A primer", *Can. J. Civil Eng.*, **36**(11), 1804-1815.
- Priestley, M.J.N. (1996), *Seismic Design and Retrofit of Bridges*, John Wiley & Sons.
- Ramsden, J. (1996), "Forces on a vertical wall due to long waves, bores, and dry-bed surges", *J. Waterw. Port C.- ASCE*, **122**(3), 134-141.
- Schultz, M.T., Gouldby, B.P., Simm, J.D. and Wibowo, J.L. (2010), Beyond the Factor of Safety: Developing Fragility Curves to Characterize System Reliability, DTIC Document
- Shinozuka, M., Feng, M.Q., Lee, J. and Naganuma, T. (2000), "Statistical analysis of fragility curves", *J. Eng. Mech. - ASCE*, **126**(12), 1224-1231.
- Spacone, E., Filippou, F.C. and Ciampi, V. (1992), *A Beam Element for Seismic Damage Analysis*, Earthquake Engineering Research Center, Berkeley, Calif.
- St-Germain, P., Nistor, I. and Townsend, R. (2012), "Numerical modeling of the impact with Structures of Tsunami bores propagating on dry and wet beds using the Sph method", *Int. J. Protective Structures*, **3**(2), 221-256.
- St-Germain, P., Nistor, I., Townsend, R. and Shibayama, T. (2014), "Smoothed-particle hydrodynamics numerical modeling of structures impacted by Tsunami bores", *J. Waterw. Port C.- ASCE*, **140**(1), 66-81.
- Taucer, F., Spacone, E., University of California, B.E.E.R.C. and Filippou, F.C. (1991), *A Fiber Beam-Column Element for Seismic Response Analysis of Reinforced Concrete Structures*, Earthquake Engineering Research Center, College of Engineering, University of California.
- Titov, V. and Gonzalez, F. (1997), *Implementation and Testing of the Method of Splitting Tsunami (Most) Model*, US Department of Commerce, National Oceanic and Atmospheric Administration, Environmental Research Laboratories, Pacific Marine Environmental Laboratory.
- Torbol, M., Gomez, H. and Feng, M. (2013), "Fragility analysis of highway bridges based on long-term monitoring data", *Comput. Aided Civil Infrastruct. E.*, **28**(3), 178-192.
- Wang, X. and Liu, P.L.F. (2006), "An analysis of 2004 Sumatra earthquake fault plane mechanisms and Indian Ocean Tsunami", *J. Hydraulic Res.*, **44**(2), 147-154.
- Yassin, M.H.M. (1994), *Nonlinear Analysis of Prestressed Concrete Structures under Monotonic and Cyclic Loads*, University of California, Berkeley.
- Yeh, H. (2007), "Design Tsunami forces for onshore structures", *J. Disaster Res.*, **2**(6), 531-536.